




The First Low-frequency Radio Observations of the Solar Corona on ≈ 200 km Long Interferometer Baseline

V. Mugundhan¹, R. Ramesh¹, C. Kathiravan¹, G. V. S. Gireesh², Anshu Kumari¹, K. Hariharan³ , and Indrajit V. Barve²

¹ Indian Institute of Astrophysics, II Block, Koramangala, Bangalore Karnataka, 560034, India

² Indian Institute of Astrophysics, Gauribidanur, Karnataka, 561210, India; mugundhan@iiap.res.in

³ National Center for Radio-Astrophysics, Ganeshkhind, Pune, 411007, India

Received 2017 December 4; revised 2018 February 1; accepted 2018 February 13; published 2018 March 1

Abstract

The angular size of the smallest, compact radio source that can be observed in the solar atmosphere is one of the intriguing questions in low-frequency radio astronomy. This is important to understand density turbulence in the solar corona and the related angular broadening of the radio source sizes. We used a two-element interferometer with a baseline length of ≈ 200 km, operating at ≈ 53 MHz to infer the above limit. Our results indicate that radio sources of angular size $\leq 15''$ exist in the solar corona, where radio emission at the above frequency also originates.

Key words: instrumentation: high angular resolution – instrumentation: interferometers – Sun: activity – Sun: corona – Sun: flares – Sun: radio radiation

1. Introduction

Irregular refraction (scattering) of radio waves due to density turbulence in the solar corona broadens the angular size of the background “radio Sun” and the compact radio sources there at any given observing frequency. But the extent of broadening and the interferometer baselines required to image the solar atmosphere in detail at radio frequencies remain a puzzle, particularly at frequencies < 100 MHz (Erickson 1964; Aubier et al. 1971; Riddle 1974; McMullin & Helfer 1977; Robinson 1983; Melrose & Dulk 1988; Subramanian & Sastry 1988; Thejappa & Kundu 1992, 1994; Sastry 1994; Schmahl et al. 1994; Ramesh & Sastry 2000; Ramesh 2000; Ramesh et al. 2001; Kathiravan et al. 2002; Bastian 2004; Subramanian 2004; Thejappa & MacDowall 2008). Past/present solar-dedicated radio imaging instruments in the above frequency range had/have limited angular resolution ($> 3'$; Wild 1967; Labrum 1972; Kundu et al. 1983; Ramesh et al. 1998). Interestingly, observations carried out during different solar eclipses (similar to the lunar occultation technique) and the bandwidth, duration of some of the solar radio transients indicate that radiowave emitting sources with angular sizes $\lesssim 1'$ are present/observable in the solar atmosphere from where radio emission at the above frequencies originate (Letfus et al. 1967; Melrose 1980; Benz & Wentzel 1981; McConnell 1983; Ramesh et al. 1999; Ramesh & Ebenezer 2001; Kathiravan et al. 2011; Ramesh et al. 2012). These are consistent with the theoretical predictions that solar radio sources of angular sizes $\lesssim 10''$ and $\lesssim 30''$ are observable at the typical frequencies of 327 MHz and 80 MHz, respectively (Riddle 1974; Subramanian & Cairns 2011). Encouraged by the above results and the availability of logistics support, we conducted interferometric observations of the solar corona at frequencies < 100 MHz on a ≈ 200 km long interferometer baseline for the first time, the description of which is the subject matter of this article.

2. Observations

We used a simple two-element correlation interferometer set-up for the observations. The center frequency of observations was 53 MHz. One “element” of the interferometer was a one-dimensional array of eight Log Periodic Dipole Antennas in the Gauribidanur Radio Observatory near Bangalore, India

(Ramesh 2011). Hereafter, we shall refer to this as Station 1. Its collecting area is ≈ 128 m². The half-power width of its response pattern is $\approx 3^\circ$ in right ascension (R.A.) and $\approx 90^\circ$ in declination (decl.). The other “element” of the interferometer was the Indian Mesospheric-Stratospheric-Tropospheric Radar near Tirupathi, India (Prasad et al. 2016). Hereafter, we shall refer to this as Station 2. It is a planar array of 1024 Yagi-Uda antenna elements with a collecting area of ≈ 16000 m². The half-power width of the response pattern is $\approx 2.5^\circ$ in both R.A. and decl. The above pattern can be steered to any desired direction in the sky within a field of view of $20^\circ \times 20^\circ$ (R.A. \times decl.) The above interferometer set-up can be considered to be a linear aperture with electric field at the edges (Kraus 1966). For such a system, the angular resolution is given by $\approx 29 \frac{\lambda}{D}^\circ$, where λ is the wavelength corresponding to the frequency of observation, and D is the length of the interferometer baseline. In the present case, $\lambda \approx 5.6$ m (53 MHz) and $D \approx 200$ km. This yields an angular resolution of $\approx 3''$. Note that considering that the local latitudes of both Stations 1 and 2 are nearly the same ($\approx 13.5^\circ$ N), the baseline between them could be considered to be oriented nearly in the east–west direction.

Identical analog and digital receivers were used for observations at both Stations 1 and 2. The antenna output in each station was band-limited using a custom made fifth-order band pass filter. The effective bandwidth of the filter was ≈ 3 MHz (i.e., ≈ 51.5 – 54.5 MHz). The output of the filter was amplified (≈ 25 dB) and then transmitted to Analog to Digital Converter (ADC). AD9284 was used as the digitizer⁴ for the recording system. The ADC was connected to a Field Programmable Gate Array (FPGA) using an interface card. The data was sampled with a clock synchronized to the 1 Pulse Per Second (1PPS) signal of a Global Positioning System Disciplined Oscillator system.⁵ The clock rates can be programmed based on trade-offs between the bandwidth of observation and the data rates. For the duration of the

⁴ <http://www.analog.com/media/en/technical-documentation/data-sheets/AD9284.pdf>

⁵ http://trl.trimble.com/docushare/dsweb/Get/Document-383329/022542-010B_Thunderbolt-E_DS_0807.pdf

experiment, the sampling frequency was maintained at 16 MHz. The sampled data was stored along with the required time information to assist in the offline correlation of the data. The data-recording was carried out via a PCI Express (PCIe) link⁶ between the FPGA and a Data Acquisition Server (DAS). A shared memory FIFO implemented on the DAS captured the recorded raw data and stored it into binary files. We verified that the system did not exhibit any data loss during the entire duration of observation. The acquired data from Stations 1 and 2 was time-aligned after compensating for the various integral and fractional delays between the radio frequency signal arrival time at the above two locations. An FX correlation routine, with temporal and spectral resolutions of ≈ 2.5 ms and ≈ 10 kHz, respectively, was implemented in MATLAB. The integration time and bandwidths are user programmable. The routine yields the cross-correlation counts, which were used for further analysis (see Mugundhan et al. 2016 for more details).

Trial observations were carried out on the radio source 3C274 during its transit over the local meridians at Stations 1 and 2. As the above source is at decl. $\approx 12^\circ 8$ N, it will be close to the local zenith at the two stations. Note that the transit time of the source at the two stations will differ by ≈ 6.6 minutes, as the longitudes of the latter are different (≈ 77.5 E for Gauribidanur, and ≈ 79.2 E for Tirupathi). We compensated for this by applying an appropriate delay in the signal path as mentioned above. While the transit of the source was detected individually at both stations, no fringes were detected on the ≈ 200 km interferometer baseline. To cross verify and understand this, we estimated the minimum detectable flux (ΔS_{\min}) for the individual stations directly from the observations. The auto-correlation profiles for 3C274 were obtained independently for Stations 1 and 2, with integration time ≈ 1 s and bandwidth ≈ 3 MHz. We used a least-squares Gaussian fitting technique to infer the peak value of the auto-correlation. We then used the fluctuations from the off-source region in the observed auto-correlation profiles to obtain the rms noise. Ratio of the above two yielded the signal-to-noise ratio (S/N) of the source. The above exercise was carried out independently for Stations 1 and 2. We set the aforementioned ratio to be the peak flux of 3C274 at 53 MHz (≈ 2700 Jy) and calculated the flux corresponding to the noise variation. The ΔS_{\min} thus estimated is ≈ 770 Jy (Station 1) and ≈ 34 Jy (Station 2). These numbers imply that ΔS_{\min} for the long baseline interferometer should be $0.5 \times \sqrt{770 \times 34}$ Jy, i.e., ≈ 80 Jy. Compared to this, the theoretical value is ≈ 10 Jy. The discrepancy could be due to issues related to the effective collecting areas of Stations 1 and 2. The system temperature could also be higher than the assumed value of 10^4 K for the theoretical calculations (Dwarakanath & Udaya Shankar 1990; Srikumar Menon et al. 2005). Observations of 3C274 reported in the literature indicate that its visibility as seen by an interferometer of length $\approx 35000\lambda$ as in the present case should be ≈ 0.005 . This implies that the corresponding flux at 53 MHz should be ≈ 13 Jy (Allen et al. 1962; Erickson et al. 1972; Clark et al. 1975). This is less than the above ΔS_{\min} for the interferometer. A survey of the existing literature indicated that the flux of the other compact radio sources, within the field of view and the sensitivity limit of the interferometer, is less than that of 3C274.

Meridian transit observations of the Sun were carried out for ≈ 1 hr every day during the period 2017 April 5–2017

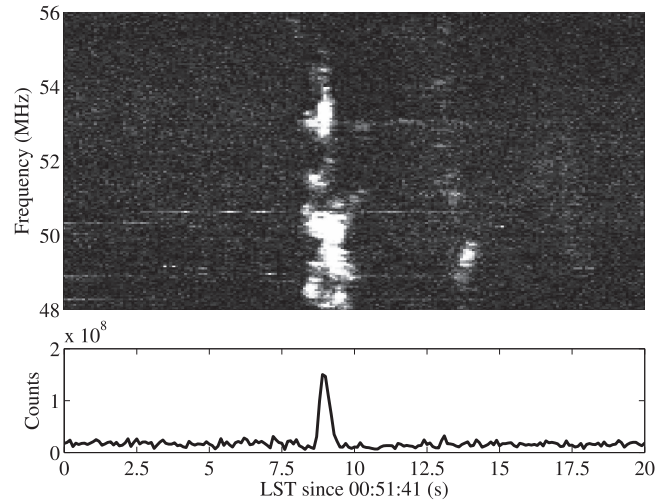


Figure 1. Upper panel: GLOSS observations of the dynamic spectrum of the transient Type IIIb solar radio burst that occurred on 2017 April 5 at $\approx 00:51:49$ LST. The integration time is ≈ 100 ms. The frequency range of the burst is ≈ 55 –48 MHz. Lower panel: time profile of the burst at 53 MHz over ≈ 100 kHz bandwidth. The duration of the burst at the above frequency is ≈ 500 ms.

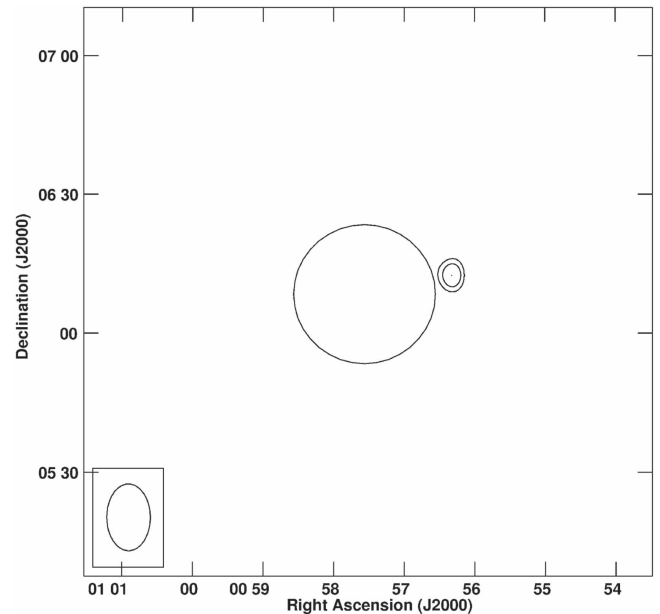


Figure 2. The location of the burst shown in Figure 1, as inferred from GRAPH observations at 53 MHz around the same epoch. The flux density of the burst at the above frequency is $\approx 32000 \pm 650$ Jy. The outer-most contour is at 90% of peak value. Solar north is straight up and east is to the left.

April 8, simultaneously at both Stations 1 and 2. The decl. of the Sun was $\approx 6.2^\circ$, close to the zenith. An inspection of the dynamic spectra obtained independently with the Gauribidanur LOW-frequency Solar Spectrograph (GLOSS; Ebenezer et al. 2001, 2007; Kishore et al. 2014) during the same epoch showed transient radio bursts from the Sun on 2017 April 5 (see Figure 1). Though the burst is patchy in frequency, there is noticeable intense emission close to ≈ 53 MHz, the center frequency of the observations with the long baseline interferometer. Similar independent observations with the Gauribidanur RadioheliograPH (GRAPH; Ramesh et al. 1998, 2006) at 53 MHz also confirmed this. The burst was located to the west limb of the Sun (Figure 2). The

⁶ <http://xillybus.com/>

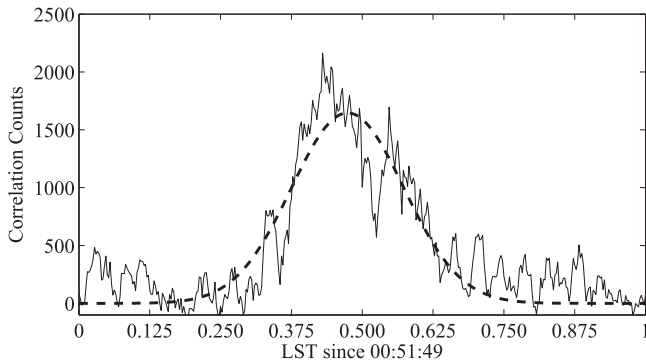


Figure 3. Variation in the cross-correlation counts obtained with the ≈ 200 km long baseline interferometer at 53 MHz during the solar radio burst in Figure 1. The “dotted” line is the Gaussian fit to the observations.

associated active region is most likely AR12645, located at W65 on the Sun that day (2017 April 5). This implies that the aforementioned radio burst is most likely due to harmonic emission, because fundamental emission from bursts near the limb will be attenuated by the overlying denser layers (see, e.g., Ramesh et al. 2010). There was no flaring activity during the burst period.⁷ Therefore, it is possible that the radio burst described above likely corresponds to the category of weak energy releases in the solar atmosphere. Low-frequency radio observations are sensitive indicators of electron acceleration associated with such energy releases (Benz 1995; Ramesh et al. 2010; Oberoi et al. 2011; Ramesh et al. 2013; Suresh et al. 2017).

Equipped with the above information, we localized the observed bursts in the independent auto-correlation spectra from Stations 1 and 2 on 2017 April 5. Subsequently, we correlated the respective raw voltage samples (corresponding to the same epoch during which the burst was noticed in the auto-correlation spectra) offline as mentioned above. Note that the visibility of a source on a particular interferometer baseline is defined as the ratio of the observed amplitude on that baseline to the observed amplitude on the “zero” baseline (i.e., the total flux from the source). In the present case, the observed cross-correlation count (i.e., ≈ 2061) on the 200 km interferometer baseline was taken to be the peak burst amplitude on that baseline. The corresponding amplitude on the “zero” baseline (estimated from the square root of the observed auto-correlation counts due to the burst at Stations 1 and 2) is ≈ 26320 . The ratio of the two (≈ 0.1) is considered as the visibility of the burst on the 200 km baseline. The system noise in the above two amplitudes is expected to be nearly the same (as it is $0.5 \times$ the square root of the product of the individual system noises in Stations 1 and 2), and hence will get canceled when we take the ratio. The profile of the burst observed with the long baseline interferometer is shown in Figure 3. The time interval of the burst (00:51:49.250 LST–00:51:49.750 LST) is the same as the period over which the burst was observed with the GLOSS (Figure 1). We repeated the correlation procedure with different delay values; however, the maximum S/N was obtained only for a particular set of delay values. This gave us confidence that the obtained correlation corresponds to the burst.

3. Analysis and Results

An inspection of the spectral observations of the burst with the GLOSS in Figure 1 indicates that they are characterized by narrow-band striae. A survey of the literature indicates that these

are Type IIIb bursts, a category of Type III bursts from the solar corona whose typical drift speeds are $\sim 0.3c$ (Ellis & McCulloch 1967; Suzuki & Dulk 1985). The peak visibility of the burst as observed with the long baseline interferometer at 53 MHz (see Figure 3) is ≈ 0.1 . This indicates that the burst source has been resolved significantly by the interferometer. A model fitting analysis was performed to estimate the source size that could give rise to the above visibility. For this, Gaussian source models of various widths were convolved with the response of the interferometer. The results indicate that a source size of $\approx 15''$ would result in the estimated visibility. This is consistent with the results of our previous similar long baseline interferometer observations, but on a ≈ 8 km baseline, in which we have shown that compact radio sources with angular size $\lesssim 1'$ could exist in regions of the corona from where 38 MHz radio emission originates (Mugundhan et al. 2016). The above source size in the present case most likely represents the width of the electron beam that generated the Type IIIb burst. The fact that coronal loop structures of angular size $\sim 20''$ can be noticed up to heliocentric distance $r \approx 2.0 R_{\odot}$ in the eclipse and coronagraph pictures of the solar corona confirms this (see, e.g., Gergely 1986).

Based on ray tracing calculations in a spherically symmetric coronal density model (including density inhomogeneities and a coronal streamer) at a typical frequency like 80 MHz, Riddle (1974) had shown that compact radio sources of angular size $\lesssim 30''$ could be observed, particularly in the case of harmonic emission from transient Type III solar radio bursts. Sources close to the solar limb are expected to be broader than those on the solar disk. McConnell (1983) had presented evidence for the presence of even smaller scale ($\approx 3''$) structures in the solar corona from where the low-frequency radio radiation originates. Subramanian & Cairns (2011) had reported source sizes $< 10''$. The recent results on density turbulence in the solar corona from low-frequency observations are also in reasonable support of the above findings (SasikumarRaja et al. 2016, 2017; Mugundhan et al. 2017). An inspection of the images obtained with the SOHO LASCO C2 coronagraph on 2017 April 5 indicates that there was a coronal streamer near the burst source in the present case, as mentioned in Riddle (1974). In consideration of these factors, the present results then clearly indicate that small-sized discrete radio sources are observable in the corona at low frequencies, provided that the observing instruments have adequate angular resolution. We also speculate that the estimated burst size of $15''$ could be an angular broadened version due to scattering and refraction effects, and the size could have been smaller if the location of the burst had been near the center of the solar disk.

4. Summary

We have reported the first long baseline (≈ 200 km) interferometer observations of the solar corona at a typical low frequency of 53 MHz in this work. Our results indicate that transient and compact solar radio sources of angular size $\leq 15''$ can be observed in the solar atmosphere from where radio emission at the above frequency originates. These results provide an indication of the smallest observable radio source sizes in the solar corona at low frequencies, and the maximum length of the interferometer baseline required to observe such fine structures. Considering that solar and heliospheric physics is one of the key science objectives for large radio interferometer arrays like LOFAR, MWA, LWA, and SKA, the present results emphasize the importance of long baselines for studying the coherent radio

⁷ <ftp://ftp.swpc.noaa.gov/pub/indices/events/20170405events.txt>

bursts associated with weak energy releases in the solar atmosphere at low frequencies ($f < 100$ MHz).

The authors would like to thank the director of NARL for providing permission to use the Indian MST Radar for the experiment. Drs. T.V.C. Sarma and A.K. Patra are thanked for their insights about the MST radar. We also thank Dr. T. R. Prasad and the Radar Applications Development Group at NARL for their help in setting up the experiment. We acknowledge the staff of the Gauribidanur radio observatory for their kind help in maintaining the antenna/receiver systems and carrying out routine observations. We thank the referee for his/her comments, which helped us to present the results more clearly.

ORCID iDs

K. Hariharan  <https://orcid.org/0000-0002-8891-8902>

References

- Allen, L. R., Anderson, B., Conway, R. G., et al. 1962, *MNRAS*, **124**, 477
 Aubier, M., Leblanc, Y., & Boischoat, A. 1971, *A&A*, **12**, 435
 Bastian, T. S. 2004, *P&SS*, **52**, 1381
 Benz, A. O. 1995, in *Coronal Magnetic Energy Releases*, Vol. 444 (Berlin: Springer), 1
 Benz, A. O., & Wentzel, D. G. 1981, *A&A*, **94**, 100
 Clark, T. A., Erickson, W. C., Hutton, L. K., et al. 1975, *AJ*, **80**, 923
 Dwarkanath, K. S., & Udaya Shankar, N. 1990, *JApA*, **11**, 323
 Ebenezer, E., Ramesh, R., Subramanian, K. R., SundaraRajan, M. S., & Sastry, C. V. 2001, *A&A*, **367**, 1112
 Ebenezer, E., Subramanian, K. R., Ramesh, R., SundaraRajan, M. S., & Kathiravan, C. 2007, *BASI*, **35**, 111
 Ellis, G. R. A., & McCulloch, P. M. 1967, *AuJPh*, **20**, 583
 Erickson, W. C. 1964, *ApJ*, **139**, 1290
 Erickson, W. C., Kuiper, T. B. H., Clark, T. A., Knowles, S. H., & Broderick, J. J. 1972, *ApJ*, **177**, 101
 Gergely, T. E. 1986, in *Proc. NRAO Workshop 10, Low Frequency Radio Astronomy*, ed. W. C. Erickson & H. V. Cane (Green Bank, WV: NRAO), 97
 Kathiravan, C., Ramesh, R., Barve, I. V., & Rajalingam, M. 2011, *ApJ*, **730**, 91
 Kathiravan, C., Ramesh, R., & Subramanian, K. R. 2002, *ApJL*, **567**, L93
 Kishore, P., Kathiravan, C., Ramesh, R., Rajalingam, M., & Barve, I. V. 2014, *SoPh*, **289**, 3995
 Kraus, J. D. 1966, *Radio Astronomy* (New York: McGraw-Hill)
 Kundu, M. R., Erickson, W. C., Gergely, T. E., Mahoney, M. J., & Turner, P. J. 1983, *SoPh*, **83**, 385
 Labrum, N. R. 1972, *SoPh*, **27**, 496
 Letfus, V., Tlamicha, A., & Valniček, B. 1967, *SoPh*, **1**, 474
 McConnell, D. 1983, *SoPh*, **84**, 361
 McMullin, J. N., & Helfer, H. L. 1977, *SoPh*, **53**, 471
 Melrose, D. B. 1980, *SoPh*, **67**, 357
 Melrose, D. B., & Dulk, G. A. 1988, *SoPh*, **116**, 141
 Mugundhan, V., Hariharan, K., & Ramesh, R. 2017, *SoPh*, **291**, 155
 Mugundhan, V., Ramesh, R., Barve, I. V., et al. 2016, *ApJ*, **831**, 154
 Oberoi, D., Matthews, L. D., Cairns, I. H., et al. 2011, *ApJL*, **728**, L27
 Prasad, T. R., Patra, A., Anandan, V., & Satyanarayana, P. 2016, *IETE Tech. Rev.*, **33**, 584
 Ramesh, R. 2000, *JApA*, **21**, 237
 Ramesh, R. 2011, *BASI*, **2**, 55
 Ramesh, R., & Ebenezer, E. 2001, *ApJL*, **558**, L141
 Ramesh, R., Kathiravan, C., Barve, I. V., Beeharry, G. K., & Rajasekara, G. N. 2010, *ApJL*, **719**, L41
 Ramesh, R., Kathiravan, C., Barve, I. V., & Rajalingam, M. 2012, *ApJ*, **744**, 165
 Ramesh, R., Kathiravan, C., Kartha, S. S., & Gopalswamy, N. 2010, *ApJ*, **712**, 188
 Ramesh, R., Kathiravan, C., & Sastry, C. V. 2001, *ApJL*, **548**, L229
 Ramesh, R., Sasikumar Raja, K., Kathiravan, C., & Satya Narayanan, A. 2013, *ApJ*, **762**, 89
 Ramesh, R., & Sastry, C. V. 2000, *A&A*, **358**, 749
 Ramesh, R., Subramanian, K. R., & Sastry, C. V. 1999, *SoPh*, **185**, 77
 Ramesh, R., Subramanian, K. R., Sundararajan, M. S., & Sastry, C. V. 1998, *SoPh*, **181**, 439
 Ramesh, R., SundaraRajan, M. S., & Sastry, C. V. 2006, *ExA*, **21**, 31
 Riddle, A. C. 1974, *SoPh*, **35**, 153
 Robinson, R. D. 1983, *PASAU*, **5**, 208
 SasikumarRaja, K., Ingale, M., Ramesh, R., et al. 2016, *JGRA*, **121**, 11605
 SasikumarRaja, K., Subramanian, P., Ramesh, R., Vourlidis, A., & Ingale, M. 2017, *ApJ*, **850**, 129
 Sastry, C. V. 1994, *SoPh*, **150**, 285
 Schmahl, E., Gopalswamy, N., & Kundu, M. R. 1994, *SoPh*, **150**, 325
 Srikumar Menon, M., Anish Roshi, D., & Rajendra Prasad, D. 2005, *MNRAS*, **356**, 958
 Subramanian, K. R. 2004, *A&A*, **426**, 329
 Subramanian, K. R., & Sastry, C. V. 1988, *JApA*, **9**, 225
 Subramanian, P., & Cairns, I. 2011, *JGRA*, **116**, A03104
 Suresh, A., Sharma, R., Oberoi, D., et al. 2017, *ApJ*, **843**, 19
 Suzuki, S., & Dulk, G. A. 1985, in *Solar Radiophysics*, ed. D. J. McLean & N. R. Labrum (Cambridge: Cambridge Univ. Press), 289
 Thejappa, G., & Kundu, M. R. 1992, *SoPh*, **140**, 19
 Thejappa, G., & Kundu, M. R. 1994, *SoPh*, **149**, 31
 Thejappa, G., & MacDowall, R. J. 2008, *ApJ*, **676**, 1338
 Wild, J. P. 1967, *PASAU*, **1**, 38